International Journal on Electrical Engineering and Informatics - Volume 16, Number 2, June 2024

Data-Driven Robust Adaptive Control Based on Synthesis of Approximating State Feedback for Robotic Manipulator

Dimitri Mahayana[1] and Sabat Anwari[2]

[1]School of Electrical Engineering and Informatics, Bandung Institute of Technology
[2]Electrotechnic Department, National Institute of Technology in Bandung

Abstract: In this research, three sequential methods are used to solve the problem of robot manipulator control. The sequentials are the feedback linearization technique, the control approach by Taylor truncation, and the data-driven robust adaptive control method. The properties of the robot manipulator are highly nonlinear, greatly time-varying, and strongly coupled. There are many uncertainties in the robot manipulator control system, such as parameter variations (e.g., inertia and payload variations), dynamically inherent effects (e.g., complicated nonlinear friction), and unmodeled behaviors. The traditional linear controllers face numerous constraints when dealing with this issue. To cope with this issue, the sliding mode control technique (SMC technique) has been popularly utilized as an accurate and robust method. Implementation of classical SMC in a system with nonlinear behavior utilizes the exact feedback linearization technique. The geometric differential theory, based on nonlinear cancellation and transformation of state variables, is employed to construct an exact linearization of a system having nonlinear input-output relations. Therefore, a classical sliding-mode controller for a linear system can be synthesized. The exact linearization has major drawbacks, i.e., its implementation is difficult. This paper demonstrates the SMC synthesis based on the state feedback approximation for controlling a robotic manipulator. The state feedback approximation is obtained using feedback with the exact linearization method. Based on the approximate state feedback, the sliding mode method is synthesized. The classical sliding mode method has major weak points limiting its practical implementation, including the chattering phenomenon and very large control input. To solve the issues, the discontinuous parts of the input parts in the classical method are substituted by a data-driven controller with a robust adaptive control method. The major advantage of this approach is that it ensures system stability without requiring understanding about uncertainty. Moreover, the converging properties and transient stability of the proposed method were examined using Lyapunov criteria. To verify the efficiency achieved by using the designed technique, a practical condition in robotic manipulator control is simulated.

Keywords: robotic manipulator, exact feedback linearization, approximating state feedback, data-driven, robust adaptive control, Lyapunov theory

1. Introduction

Due to the ability of the robotic manipulator to pick up, move, and drop objects, manipulate objects and tools, and explore three-dimensional space, in the field of material handling operations in the manufacturing process, the first choice is to use a robotic manipulator system. Modern industrial automation, such as in manufacturing, requires robotic manipulators in the fields of material handling, processing operations, as well as assembly and inspection.

Recently, robotic manipulators have been widely utilized in the automation industry because they can replace the function of human arms, which are equipped with artificial intelligence. These mechanical devices require high speed and high precision performance; therefore, research on better control systems is needed. This high-performance control system usually requires a mathematical model of the robotic manipulator to design the controller systematically by using a simulation approach [1].

The robot manipulator has high nonlinearity, great coupling, and time-varying characteristics. In fact, the mathematical models always contain uncertainties, including external

Received: July 11st, 2023. Accepted: June 24th, 2024
DOI: 10.15676/ijeei.2024.16.2.7

perturbations, unmodeled parameter unpredictability, sensor faults, and others, which ultimately lead to instability [2]–[8].

Over the last few decades, various control system design approaches, such as robust control method [9],optimal method [10]–[12],adaptive method [13],backstepping method [14], adaptive backstepping method [15], adaptive neural backstepping method [16], adaptive RBF neural network backstepping method[17],backstepping-based super-twisting sliding mode method [18], adaptive backstepping sliding mode method [19], fuzzy logic [20], sliding mode method [6], neural network [21], and neural adaptive robust method [22]for robotic manipulator control have been submitted.

In the last few years, much attention has been paid to the application of data-driven control to robotic manipulator control. Fortunately, the digital control of a robotic manipulator can produce large amounts of input and output (I/O) measurement data that contain all the state information. This shows that a data-driven controller can be developed without the modeling process. There are several data-driven control methods that are proposed for use in robotic manipulator control, including model predictive control [23]–[26], the Gaussian process regression method [13], statistical models [27], neural PID [28], passivity based control [29], and unfalsified control [30].

Linearization using feedback is a method for nonlinear control systems that has generated many papers in the past few year ([3], [31]–[33]). The main point is to mathematically change nonlinear a nonlinear model to a linear model (completely or partially) so that a control system can be synthesized using the linear method. In classical exact linearization using feedback, coordinate changes and static feedback are used such that the closed-loop form of the system, at a given limit, generates a linear a linear system in canonical form. After the linearization form of the system is acquired, the synthesis is carried out utilizing linear control techniques to accomplish a stable tracking or regulatory system [34], [35].

In exact linearization using the feedback mentioned above, the controller properties have nonlinear functions such as the state variables multiplications, polynomial properties, trigonometric properties, and others, so it is very difficult to implement the controller in the form of electronic devices [36]–[39]. On the contrary, the performance of the controller has been proven to be able to maintain a good response even though the approximate feedback linearization technique has been utilized [40], [41].

In order to synthesize a nonlinear control system, in the research of Mahayana [3], [42], a methodology was developed that makes the realization of a linearization controller more realistic without a significant degradation in performance. In the study, the developed controller was not based on an exact linearization controller but on the development of an exact linearization method in the form of a linear feedback system, which can replace the exact linearization controller function. Examination of the stability of the closed-loop control system, which is controlled using the proposed controller utilizing Lyapunov's criterion theory. The characteristic value shift theorem is used to form the origin condition in the stable region so that as a whole it produces an asymptotically stable closed loop control system. As far as we know, no other authors have utilized the method to design a controller for a plant.

In previous research [3], gravity on the robotic manipulator was ignored; however, the presence of gravity produces a non-zero steady-state error and will degrade the performance of the control system. Non-zero steady-state error cannot be assured if using controllers based on approximate state feedback. To enhance the previous studies, a data-driven, robust adaptive control method for controlling a robotic manipulator system was synthesized in two steps. The first step is to design approximate state feedback based on an exact linearization method. The second step is to synthesize a data-driven controller based on the adaptive proportional integral (PI) method to deal with unpredictability in the control system. Accurate tracking capability and robust performance are shown in the simulation results.

2. Dynamics of Robotic Manipulator

In this paper, to ease the problem, we use a two-joint robot manipulator as depicted in Figure 1 [43]. In Figure 1, m_1 and m_2 are masses of arm1 and arm2 respectively; l_1 and l_2 are lengths of arm1 and arm2; t_1 and t_2 are torque on arm1 and arm2; θ_1 and θ_2 are positions of arm1 and arm2. The dynamical behavior of a two-joint robotic manipulator model can be expressed in the form of a mathematical formula as follows:

$$\boldsymbol{M}(\boldsymbol{q})\ddot{\boldsymbol{q}} + \boldsymbol{B}(\boldsymbol{q},\dot{\boldsymbol{q}})\dot{\boldsymbol{q}} + \boldsymbol{G}(\boldsymbol{q}) = \boldsymbol{T} \tag{1}$$

where $\boldsymbol{q} = [\theta_1 \quad \theta_2]^T$ denotes the joint position vector; $\boldsymbol{M}(\boldsymbol{q}) \in \mathfrak{R}^{nxn}$ stands for the moment of inertia; $\boldsymbol{B}(\boldsymbol{q},\dot{\boldsymbol{q}})\dot{\boldsymbol{q}}$ are matrices indicating the Coriolis and centripetal forces; $\boldsymbol{G}(\boldsymbol{q})$ contains the gravitational forces; $\boldsymbol{T} = [t_1 \quad t_2]^T$ is the input vector, which is the applied torque.

Let $c_i \equiv cos \ \theta_i$, $c_{ij} \equiv cos(\theta_i + \theta_j)$, then $\boldsymbol{M}, \boldsymbol{B}, \boldsymbol{G}$ in (1) can be written as follows:

$$\begin{aligned} \boldsymbol{M}(\boldsymbol{q}) &= \begin{bmatrix} m_{11} & m_{12} \\ m_{21} & m_{22} \end{bmatrix}, \\ \boldsymbol{B}(\boldsymbol{q},\dot{\boldsymbol{q}}) &= \begin{bmatrix} b_{11} & b_{12} \\ b_{21} & b_{22} \end{bmatrix}, \\ \boldsymbol{G}(\boldsymbol{q}) &= \begin{bmatrix} (m_1+m_2)l_1 g c_2 + m_2 l_2 g c_{12} \\ m_2 l_2 g c_{12} \end{bmatrix}, \end{aligned} \tag{2}$$

where:

$$\begin{aligned} m_{11} &= (m_1+m_2)l_1^2 + m_2 l_2^2 + 2m_2 l_1 l_2 c_2, \\ m_{12} &= m_{21} = m_2 l_2^2 + m_2 l_1 l_2 c_2, \\ m_{22} &= m_2 l_2^2, \\ b_{11} &= -m_2 l_1 l_2 \dot{\theta}_2 \sin \ \theta_2, \\ b_{12} &= -m_2 l_1 l_2 (\dot{\theta}_1 + \dot{\theta}_2) \sin \ \theta_2, \\ b_{21} &= m_2 l_1 l_2 \dot{\theta}_1 \sin \ \theta_2, \\ b_{22} &= 0. \end{aligned}$$

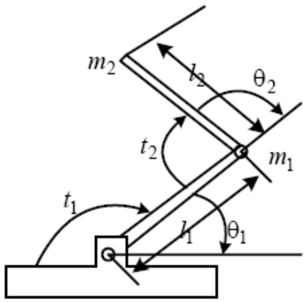

Figure 1. Structure of Two-Joints Robotic Manipulator

The robot inertial matrix, $\boldsymbol{M}(\boldsymbol{q})$, is a symmetric matrix as well as positive definite. The boundedness of the robot inertial matrix as a function of $\boldsymbol{q} : \mu_1 \boldsymbol{I} \leq \boldsymbol{M}(\boldsymbol{q}) \leq \mu_2 \boldsymbol{I}$, can be proven. $\dot{\boldsymbol{M}}(\boldsymbol{q}) - 2\boldsymbol{B}(\boldsymbol{q},\dot{\boldsymbol{q}})$ is a matrix of size $n \times n$ and skew-symmetric, that is, with the nonzero vector $\boldsymbol{x} \in \mathfrak{R}^{nx1}, \boldsymbol{x}^T[\dot{\boldsymbol{M}}(\boldsymbol{q}) - 2\boldsymbol{B}(\boldsymbol{q},\dot{\boldsymbol{q}})] \ \boldsymbol{x} = 0$ is obtained.

Let us define the input $\boldsymbol{u} = \boldsymbol{T}$ and the state variable $\boldsymbol{x} = [x_1 \quad x_2 \quad x_3 \quad x_4]^T = [\theta_1 \quad \dot{\theta}_1 \quad \theta_2 \quad \dot{\theta}_2]^T$. The behavioral equation for the movement of the robot manipulator model can be described in the form of a state-space nonlinear mathematical formula as follows:

$$\dot{\boldsymbol{x}} = \boldsymbol{f}(\boldsymbol{x}) + \boldsymbol{g}(\boldsymbol{x})\boldsymbol{u}, \tag{3}$$

where $\boldsymbol{f}(\boldsymbol{x})$ is a continuous and nonlinear function having an upper bound formulated as $|\boldsymbol{f}(\boldsymbol{x})| \leq \bar{\boldsymbol{f}}$, and $\boldsymbol{g}(\boldsymbol{x})$ is a function describing the gain with a lower bound formulated as $\underline{\boldsymbol{g}}$, $0 < \underline{\boldsymbol{g}} < \boldsymbol{g}(\boldsymbol{x})$.

3. Controller Synthesis

A. Matrix Norm and Spectral Radius

Definition 1. [44], [45] If $\boldsymbol{A} \in \boldsymbol{C}^{nxn}$, then the definition of the spectral norm of matrix $\boldsymbol{A}$ is represented as follows:

$$\|\boldsymbol{A}\|_s \stackrel{\text{def}}{=} \sup_{\boldsymbol{w} \in \boldsymbol{C}^n} \frac{\|\boldsymbol{A}\boldsymbol{w}\|_2}{\|\boldsymbol{w}\|_2}. \quad (4)$$

Definition 2. [44], [45] The spectral radius of the square matrix $\boldsymbol{A} \in \boldsymbol{C}^{nxn}$, $\rho(\boldsymbol{A})$, is described as the largest absolute value of the spectral elements of matrix $\boldsymbol{A}$ or its eigenvalues.

To calculate the values of the spectral square matrix norm, start with Lancaster and Tismenetsky [45]:

$$\|\boldsymbol{A}\|_s = \left(\rho(\boldsymbol{A}\boldsymbol{A}^*)\right)^{\frac{1}{2}}, \quad (5)$$

where subscript $*$ denotes the conjugate transpose of a matrix.

B. Lyapunov Theory and Linearization

Examine the following system, which is nonlinearly structured:

$$\dot{\boldsymbol{x}} = \boldsymbol{f}(\boldsymbol{x}), \quad (6)$$

with $\boldsymbol{f}(\boldsymbol{0}) = \boldsymbol{0}$, or in another way, the origin of system is the equilibrium point, and the vector field $\boldsymbol{f}$ is globally continuous and at the least one-time differentiable with respect to $\boldsymbol{x}$, then a linear time-invariant system can be used to approximate a nonlinear system represented as the following formula:

$$\dot{\boldsymbol{x}} = \Psi \boldsymbol{x}, \quad (7)$$

$$\Psi \stackrel{\text{def}}{=} \left.\frac{\partial \boldsymbol{f}}{\partial \boldsymbol{x}}\right|_{\boldsymbol{x}=\boldsymbol{0}}, \quad (8)$$

where $\Psi \in \mathfrak{R}^{nxn}$ is a constant matrix.

Theorem 1 [46], [47] If the system (7), which is the result of linearization, has an asymptotically stable origin($\boldsymbol{x} = \boldsymbol{0}$), then the nonlinear system in Equation (6) will also have an asymptotically stable origin.

C. The Method of Shifting Characteristic Values

The derivation of the sufficient conditions so that a closed-loop system using an exact controller can produce an asymptotically stable origin will be discussed in this sub-section. Let the controller candidate be defined as follows:

$$\boldsymbol{u}_a \stackrel{\text{def}}{=} \boldsymbol{u}_a(\boldsymbol{x}), \quad (9)$$

and $\boldsymbol{u}_a(\boldsymbol{x})$ at least one-time differentiable with respect to $\boldsymbol{x}$ and $\boldsymbol{u}_a(\boldsymbol{0}) = \boldsymbol{u}(\boldsymbol{0})$.

Between "exact controller" and "controller candidate", there is an error that can be formulated as follows:

$$\boldsymbol{e}(\boldsymbol{x}) = \boldsymbol{u}_a(\boldsymbol{x}) - \boldsymbol{u}(\boldsymbol{x}). \quad (10)$$

Assume a notation:

$$\boldsymbol{A}_c = \boldsymbol{A} + \boldsymbol{B}\boldsymbol{K}, \quad (11)$$

with the matrix of a closed-loop system using the exact controller formulated with $\boldsymbol{A}_c$, and, respectively, several variables are also defined as follows:

$$\upsilon(\boldsymbol{A}_c) \stackrel{\text{def}}{=} \inf_{\boldsymbol{P}}(\|\boldsymbol{P}^{-1}\|_s \|\boldsymbol{P}\|_s), \quad (12)$$

$$\boldsymbol{\varepsilon}(\boldsymbol{x}) \stackrel{\text{def}}{=} \left(L_{\boldsymbol{g}} L_{\boldsymbol{f}}^{n-1} \boldsymbol{T}_1(\boldsymbol{x})\right) \boldsymbol{e}(\boldsymbol{x}), \quad (13)$$

$$\kappa \stackrel{\text{def}}{=} \left\| \left(\left(\frac{\partial \boldsymbol{\varepsilon}(\boldsymbol{x})}{\partial \boldsymbol{x}}\right)^T \left(\nabla \boldsymbol{T}(\boldsymbol{x})\right)^{-1}\Big|_{\boldsymbol{x}=\boldsymbol{0}} \right)^T \right\|, \quad (14)$$

with a transformation matrix, $\boldsymbol{P}$, which transforms matrix $\boldsymbol{A}_c$ into a diagonal canonical matrix as follows:

$$\boldsymbol{P}\boldsymbol{A}_c\boldsymbol{P}^{-1} = diag(\lambda_1,\ \lambda_1, \cdots,\ \lambda_n), \quad (15)$$

with $\boldsymbol{A}_c$, i.e., a closed-loop matrix using an exact controller, has characteristic values formulated with $\lambda_1,\ \lambda_1,\cdots,\ \lambda_n$, while the shortest distance of the characteristic value to the imaginary axis is denoted by λ_c (assuming that all characteristic values strictly lie to the left of the imaginary axis of the complex plane).

The exact linear transformation results in a linear time-invariant (LTI) system, namely the matrix pair $(\boldsymbol{A}, \boldsymbol{B})$, which has the Brunovosky canonical form; therefore, the matrix in a closed-loop system can be designed to have characteristic values that are all different. To realize this, Chen [48]used the pole placement technique. It is necessary to take the assumption of different values of $\boldsymbol{A}_c$ characteristics so that the transformation of the matrix $\boldsymbol{A}_c$ to a pure diagonal form can be carried out [45], [49].

Theorem 2. If

$$Re(\lambda_c) + \kappa \boldsymbol{v}(\boldsymbol{A}_c) < 0, \tag{16}$$

then the nonliner system (3) controlled using $\boldsymbol{u}_a(\boldsymbol{x})$ will produce an asymptotically stable origin.

Proof. The proof of Theorem 2 requires several stages: first stage, synthesizing the system using an exact controller; second stage, proving the existence of candidate controllers; third stage, carrying out the process of transforming the system controlled using the candidate controller into a new state-space form; fourth stage, proving the stability of the system using Lyapunov criteria; and fifth stage, carrying out the process of analyzing the values of the shift characteristic.

D. Construction Under Exact Controller

In order for Equation (1) to be linear, it is necessary to choose $\boldsymbol{T}$ exactly. Adopted from Slotine and Li [35], the formula for $\boldsymbol{T}$ can be represented as follows:

$$\boldsymbol{T} = \boldsymbol{M}(\boldsymbol{q})\boldsymbol{v} + \boldsymbol{B}(\boldsymbol{q}, \dot{\boldsymbol{q}})\dot{\boldsymbol{q}} + \boldsymbol{G}(\boldsymbol{q}), \tag{17}$$

where $\boldsymbol{v} \in \mathfrak{R}^{2x1}$ is the system input involving the linearization process, leading to:

$$\ddot{\boldsymbol{q}} = \boldsymbol{v}. \tag{18}$$

By describing the selected state variable as $\boldsymbol{x} = [x_1 \quad x_2 \quad x_3 \quad x_4]^T = [\theta_1 \quad \dot{\theta}_1 \quad \theta_2 \quad \dot{\theta}_2]^T$, it can be proven that the robotic manipulator control system can be written in the Brunovsky canonical formula as follows:

$$\dot{\boldsymbol{x}} = \begin{bmatrix} 0 & 1 & 0 & 0 \\ 0 & 0 & 0 & 0 \\ 0 & 0 & 0 & 1 \\ 0 & 0 & 0 & 0 \end{bmatrix} \boldsymbol{x} + \begin{bmatrix} 0 & 0 \\ 1 & 0 \\ 0 & 0 \\ 0 & 1 \end{bmatrix} \boldsymbol{v}. \tag{19}$$

By defining $\boldsymbol{z}_i = \left[\theta_i\ \dot{\theta}_i\right]^T, i = 1,2$; the distribution of Equation (19) in two subsystems in a linear form will be represented as follows:

$$\dot{\boldsymbol{z}}_i = \begin{pmatrix} 0 & 1 \\ 0 & 0 \end{pmatrix} \boldsymbol{z}_i + \begin{pmatrix} 0 \\ 1 \end{pmatrix} v_i. \tag{20}$$

Letting:

$$v_i = -\vartheta_{n,i}^2 \varsigma_i - 2\xi_i \vartheta_{n,i}\, \dot{\varsigma}_i, \tag{21}$$

where $\vartheta_{n,i} \in \mathfrak{R}$ denotes $i-th$ natural frequency, ξ_i denotes $i-th$ damping ratio, and $i = 1,2$.

The ITAE performance criterion for a system with a step input can be minimized utilizing the pole-placement method so that the overall system has a damping ratio of $\xi_i = 0.707$, and the $i-th$ natural frequency can be designed as follows:

$$\begin{aligned} \vartheta_{n,1} &= 15, \\ \vartheta_{n,2} &= 16, \end{aligned} \tag{22}$$

The calculation of the value of the feedback gain, $\boldsymbol{K}$, is done with the following representation:

$$\boldsymbol{K}^T = \begin{bmatrix} -225 & 0 \\ -21.21 & 0 \\ 0 & -256 \\ 0 & -22.624 \end{bmatrix}. \tag{23}$$

E. Existence of Controller Candidate

The transformation, $\boldsymbol{T}: \boldsymbol{\Omega} \rightarrow \boldsymbol{T}(\boldsymbol{\Omega}) \subset \Re^n$, with $\boldsymbol{\Omega}$ being an open set on the domain, $\Re^n$, is guaranteed to be a dipheomorphism; therefore, it can be concluded that $\boldsymbol{T}$ is smooth. As a result, the smoothness of $\boldsymbol{u}(\boldsymbol{x})$ can be guaranteed. Since $\boldsymbol{u}(\boldsymbol{x})$ is smooth, the design of the new control input, i.e., $\boldsymbol{u}_a(\boldsymbol{x})$, can be chosen to be continuous, and the function on $\boldsymbol{u}_a(\boldsymbol{x})$ is at least one-time differentiable with respect to $\boldsymbol{x}$, fulfilling $\boldsymbol{u}_a(\boldsymbol{0}) = \boldsymbol{u}(\boldsymbol{0})$, and it satisfies:

$$\|\boldsymbol{u}_a(\boldsymbol{x}) - \boldsymbol{u}(\boldsymbol{x})\|_\infty \leq \delta, \tag{24}$$

where δ is a positive real constant, over the range $\boldsymbol{\nu} \subset \boldsymbol{\Omega} \subset \Re^n$, whit $\boldsymbol{\nu}$ is a closed and bounded set.

F. System Transformation under Controller Candidate

The representation of a dynamical system that is nonlinear with the manipulated variable, $\boldsymbol{u}_a(\boldsymbol{x})$, can be described as follows:

$$\dot{\boldsymbol{x}} = \boldsymbol{f}(\boldsymbol{x}) + \boldsymbol{g}(\boldsymbol{x})\boldsymbol{u}_a(\boldsymbol{x}). \tag{25}$$

Equation (25) can be arranged as follows:

$$\dot{\boldsymbol{x}} = \boldsymbol{f}(\boldsymbol{x}) + \boldsymbol{g}(\boldsymbol{x})\{\boldsymbol{u}(\boldsymbol{x}) + \boldsymbol{e}(\boldsymbol{x})\}. \tag{26}$$

By going through several complicated calculation stages, the representation of Equation (26) can be described in the form of a new state variable, $\boldsymbol{z}$, with the following formula:

$$\dot{\boldsymbol{z}} = \boldsymbol{A}_c\boldsymbol{z} + \begin{bmatrix} 0 \\ 0 \\ \vdots \\ 1 \end{bmatrix} \boldsymbol{\varepsilon}\{\boldsymbol{T}^{-1}(\boldsymbol{z})\}. \tag{27}$$

The mathematical representation of the overall system using a controller candidate in the form of a state-space with new coordinates can be represented by a nonlinear system, which is a combination of linear subsystems and nonlinear perturbation subsystems.

By designing $\boldsymbol{u}_a(\boldsymbol{x})$ in such a way that it results in $\boldsymbol{u}_a(\boldsymbol{0}) = \boldsymbol{u}(\boldsymbol{0}) = \boldsymbol{0}$, this would imply $\boldsymbol{e}(\boldsymbol{0}) = \boldsymbol{0}$, consequently at $\boldsymbol{z} = \boldsymbol{0}$,

$$\boldsymbol{A}_c\boldsymbol{z} + \begin{bmatrix} 0 \\ 0 \\ \vdots \\ 1 \end{bmatrix} \boldsymbol{\varepsilon}\{\boldsymbol{T}^{-1}(\boldsymbol{z})\} = \boldsymbol{0}. \tag{28}$$

This indicates that the overall system equilibrium point using a controller candidate is the same as the overall system equilibrium point using an exact controller.

G. Lyapunov Stability Analysis

Equation (27), which is a nonlinear system, can be described using the following formula:

$$\dot{\boldsymbol{z}} = \boldsymbol{f}_c(\boldsymbol{z}), \tag{29}$$

with

$$\boldsymbol{f}_c(\boldsymbol{z}) = \boldsymbol{A}_c\boldsymbol{z} + \begin{bmatrix} 0 \\ 0 \\ \vdots \\ 1 \end{bmatrix} \boldsymbol{\varepsilon}\{\boldsymbol{T}^{-1}(\boldsymbol{z})\}. \tag{30}$$

The $\boldsymbol{f}_c(\boldsymbol{z})$ is a function that is smooth around the origin; therefore, it will produce $\frac{\partial \boldsymbol{f}_c(\boldsymbol{z})}{\partial \boldsymbol{z}}$, which exists around the origin. Based on Equation (28), it can be proven that the origin is an equilibrium point, and this can be expressed in the following formula:

$$\boldsymbol{f}_c(\boldsymbol{0}) = \boldsymbol{0}. \tag{31}$$

The system linearization process in Equation (29) around the origin can be described in the form of the following formula:

$$\dot{\boldsymbol{z}} = \left.\frac{\partial \boldsymbol{f}_c(\boldsymbol{z})}{\partial \boldsymbol{z}}\right|_{\boldsymbol{z}=\boldsymbol{0}} * \boldsymbol{z}. \tag{32}$$

Equation (32) can be described in the form of the following formula:

$$\dot{\boldsymbol{z}} = (\boldsymbol{A}_c + \boldsymbol{D})\boldsymbol{z}, \tag{33}$$

with

$$\boldsymbol{D} = \left[\begin{array}{c} \boldsymbol{O}_{(n-1)\times n} \\ \hline \left(\frac{\partial \boldsymbol{\varepsilon}(\boldsymbol{x})}{\partial \boldsymbol{x}}\right)^T \left(\nabla \boldsymbol{T}(\boldsymbol{x})\right)^{-1}\Big|_{\boldsymbol{x}=\boldsymbol{0}} \end{array} \right]. \tag{34}$$

Lyapunov states in his stability theory that if the system origin in Equation (33) can be proven to be asymptotically stable, then the origin of the system in Equation (29) which in this case is a closed loop system with a newly designed controller, i.e., the controller candidate, $\boldsymbol{u}_a(\boldsymbol{x})$, can also be proven to be asymptotically stable. This system can be proven to be stable if all the spectral values or eigenvalues of the matrix, $(\boldsymbol{A}_c + \boldsymbol{D})$, are designed to be strictly placed on the left of the complex plane.

H. Analysis of Shifting Characteristic Values

The representation of the linear system described in Equation (33) can be expressed as the sum of two matrices, i.e., the nominal matrix, $\boldsymbol{A}_c$, and the matrix indicating perturbation, $\boldsymbol{D}$. The eigenvalues of the matrix$(\boldsymbol{A}_c + \boldsymbol{D})$are assumed to be $\zeta_1, \zeta_2, \cdots, \zeta_n$, and further from the definition of the eigenvalue [44], [45], the relationship between the matrix and its eigenvalues can be represented as the following formula:

$$(\boldsymbol{A}_c + \boldsymbol{D})\boldsymbol{y}_i = \zeta_i \boldsymbol{y}_i,\ \exists \boldsymbol{y}_i \neq \boldsymbol{0},\ \boldsymbol{y}_i \in \boldsymbol{C}^n. \tag{35}$$

Assume $\boldsymbol{A}_c = \boldsymbol{P}\boldsymbol{A}_{c_D}\boldsymbol{P}^{-1}$, with $\boldsymbol{A}_{c_D} = diag(\lambda_1, \lambda_2, \cdots, \lambda_n)$. Equation (35) can be represented as the following formula:

$$\left(\boldsymbol{A}_{c_D} + \boldsymbol{P}^{-1}\boldsymbol{D}\boldsymbol{P}\right)\boldsymbol{r}_i = \zeta_i \boldsymbol{r}_i, \tag{36}$$

with $\boldsymbol{r}_i = \boldsymbol{P}^{-1}\boldsymbol{y}_i \neq \boldsymbol{0}$. After a little manipulation, it can be found:

$$\left(\zeta_i \boldsymbol{I} - \boldsymbol{A}_{c_D}\right)\boldsymbol{r}_i = \boldsymbol{P}^{-1}\boldsymbol{D}\boldsymbol{P}. \tag{37}$$

After some complicated calculations, we can find:

$$\frac{\left\|\left(\zeta_i \boldsymbol{I} - \boldsymbol{A}_{c_D}\right)\boldsymbol{r}_i\right\|_2}{\|\boldsymbol{r}_i\|_2} \leq \upsilon(\boldsymbol{A}_c)\|\boldsymbol{D}\|_2. \tag{38}$$

Since:

$$\|\boldsymbol{D}\|_2 = \{\rho(\boldsymbol{D}\boldsymbol{D}^*)\}^{\frac{1}{2}} = \kappa, \tag{39}$$

then:

$$\frac{\left\|\left(\zeta_i \boldsymbol{I} - \boldsymbol{A}_{c_D}\right)\boldsymbol{r}_i\right\|_2}{\|\boldsymbol{r}_i\|_2} \leq \upsilon(\boldsymbol{A}_c)\kappa. \tag{40}$$

If λ_{ci} is one of the eigenvalues of matrix $\boldsymbol{A}_c$ whose distance to ζ_i is assumed to be the shortest, then:

$$|\zeta_i - \lambda_{ci}| \leq \frac{\left\|\left(\zeta_i \boldsymbol{I} - \boldsymbol{A}_{c_D}\right)\boldsymbol{r}_i\right\|_2}{\|\boldsymbol{r}_i\|_2} \leq \upsilon(\boldsymbol{A}_c)\kappa. \tag{41}$$

I. Construction of Controller Candidate

The robotic manipulator used in this study uses the following parameter values: $m_1 = 4\ kg$, $m_2 = 2\ kg$, $l_1 = 1\ m$, $l_2 = 0.5\ m$, and $g = 9.8\ N/kg$.

The proposed controller candidate can be described using the following formula:

$$\boldsymbol{u}_a(\boldsymbol{x}) = \boldsymbol{L}\boldsymbol{x}, \tag{42}$$

where $\boldsymbol{L} \in \mathfrak{R}^{2x4}$.

From the equations that have been derived, the error between a system controlled using an exact controller and a system controlled using an approximating controller can be described using the following formula:

$$\boldsymbol{e}(\boldsymbol{x}) = -\boldsymbol{\alpha}(\boldsymbol{x}) - \boldsymbol{\beta}(\boldsymbol{x})\boldsymbol{K}\boldsymbol{z}(\boldsymbol{x}) + \boldsymbol{L}\boldsymbol{x}, \tag{43}$$

where:

$$\boldsymbol{\alpha}(\boldsymbol{x}) = \boldsymbol{B}(\boldsymbol{q},\ \dot{\boldsymbol{q}})\ \dot{\boldsymbol{q}} + \boldsymbol{G}(\boldsymbol{q}),$$
$$\boldsymbol{\beta}(\boldsymbol{x}) = \boldsymbol{M}(\boldsymbol{q}).$$

Based on (43). It found:

$$\boldsymbol{\varepsilon}(\boldsymbol{x}) = \boldsymbol{\beta}^{-1}(\boldsymbol{x})\boldsymbol{e}(\boldsymbol{x}). \tag{44}$$

After some complicated calculations, we can find:

$$\boldsymbol{\varepsilon}(\boldsymbol{x}) = \begin{bmatrix} \varepsilon_1(\boldsymbol{x}) \\ \varepsilon_2(\boldsymbol{x}) \end{bmatrix}, \tag{45}$$

where:

$$\varepsilon_1(\boldsymbol{x}) = \frac{0.5 + \cos\ x_3}{3 - \cos^2 x_3}\alpha_2 - \boldsymbol{K}_1\boldsymbol{x} - \frac{0.5}{3 - \cos^2 x_3}(\alpha_{11} + \alpha_{12}) + \frac{0.5\boldsymbol{L}_1\boldsymbol{x} - (0.5 + \cos x_3)\boldsymbol{L}_2\boldsymbol{x}}{3 - \cos^2 x_3}, \tag{46}$$

and:

$$\varepsilon_2(x) = \frac{0.5 + \cos x_3}{3 - \cos^2 x_3}(\alpha_{11} + \alpha_{12}) - \frac{6.5 + 2\cos x_3}{3 - \cos^2 x_3}\alpha_2 - \boldsymbol{K}_2\boldsymbol{x} - \frac{(0.5 + \cos x_3)\boldsymbol{L}_1\boldsymbol{x}}{3 - \cos^2 x_3} + \frac{(6.5 + 2\cos x_3)\boldsymbol{L}_2\boldsymbol{x}}{3 - \cos^2 x_3}, \tag{47}$$

with:

$$\begin{aligned} \alpha_{11} &= -2x_2x_4 \sin x_3 - x_4^2 \sin x_3, \\ \alpha_{12} &= 58.8 \cos x_3 + 9.8\cos(x_1 + x_3), \\ \alpha_2 &= x_2^2 \sin x_3 + 9.8\cos(x_1 + x_3), \\ \boldsymbol{K}_1 &= [K_{11} \quad K_{12} \quad K_{13} \quad K_{14}], \\ \boldsymbol{K}_2 &= [K_{21} \quad K_{22} \quad K_{23} \quad K_{24}], \\ \boldsymbol{L}_1 &= [L_{11} \quad L_{12} \quad L_{13} \quad L_{14}], \\ \boldsymbol{L}_2 &= [L_{21} \quad L_{22} \quad L_{23} \quad L_{24}]. \end{aligned} \tag{48}$$

If we differentiate $\boldsymbol{\varepsilon}(\boldsymbol{x})$ with respect to $\boldsymbol{x}$ and assign the value of $\boldsymbol{x} = \boldsymbol{0}$, the following equations will result:

$$\begin{aligned} \frac{\partial \varepsilon_1}{\partial x_1} &= 225 + \frac{0.5L_{11} - 1.5L_{21}}{2}, \\ \frac{\partial \varepsilon_1}{\partial x_2} &= 21.21 + \frac{0.5L_{12} - 1.5L_{22}}{2}, \\ \frac{\partial \varepsilon_1}{\partial x_3} &= \frac{0.5L_{13}}{3} - \frac{1.5L_{23}}{3}, \\ \frac{\partial \varepsilon_1}{\partial x_4} &= \frac{0.5L_{14} - 1.5L_{24}}{2}, \\ \frac{\partial \varepsilon_2}{\partial x_1} &= \frac{8.5L_{21} - 1.5L_{11}}{2}, \\ \frac{\partial \varepsilon_2}{\partial x_2} &= \frac{8.5L_{22} - 1.5L_{12}}{2}, \\ \frac{\partial \varepsilon_2}{\partial x_3} &= 256 + \frac{8.5L_{23} - 1.5L_{13}}{2}, \\ \frac{\partial \varepsilon_2}{\partial x_4} &= 22.624 + \frac{8.5L_{24} - 1.5L_{14}}{2}. \end{aligned} \tag{49}$$

If we select:

$$\boldsymbol{L}^T = \begin{bmatrix} -1912.5 & -337.5 \\ -180.285 & -31.815 \\ -384 & -128 \\ -33.936 & -11.312 \end{bmatrix}, \tag{50}$$

will imply:

$$\left.\frac{\partial \boldsymbol{\varepsilon}}{\partial \boldsymbol{x}}\right|_{\boldsymbol{x}=\boldsymbol{0}} = \boldsymbol{0}, \tag{51}$$

and furthermore, this will imply:

$$\kappa = \left\| \left(\left(\frac{\partial \boldsymbol{\varepsilon}(\boldsymbol{x})}{\partial \boldsymbol{x}} \right)^T (\nabla \boldsymbol{T}(\boldsymbol{x}))^{-1}|_{\boldsymbol{x}=\boldsymbol{0}} \right)^T \right\| = 0. \tag{52}$$

In this case, $\kappa = 0$, so it can be concluded that Equation (16) is always fulfilled; furthermore, we can guarantee that the origin of the closed-loop system (1), which is controlled using controller:

$$\boldsymbol{u}_a(\boldsymbol{x}) = \begin{bmatrix} -1912.5 & -337.5 \\ -180.285 & -31.815 \\ -384 & -128 \\ -33.936 & -11.312 \end{bmatrix}^T \boldsymbol{x}, \tag{53}$$

$$\boldsymbol{u}_a(\boldsymbol{x}) = \begin{bmatrix} -1912.5 & -337.5 \\ -180.285 & -31.815 \\ -384 & -128 \\ -33.936 & -11.312 \end{bmatrix}^T \boldsymbol{x}, \tag{54}$$

will be asymptotically stable.

J. Data-Driven Robust Adaptive Controller

The robotic manipulator system, which is controlled using an approximating state feedback controller, has the main disadvantage, i.e., the existence of a steady state error due to gravity. The drawbacks that have been discussed previously led to the idea of adding a data-driven robust adaptive controller to a system that is controlled using the approximating state feedback method. The first step to designing the controller, the definition of the tracking error, is represented as follows:

$$e_i = \theta_{di} - \theta_i, \tag{55}$$

where θ_{di} is the desired trajectory of θ_i. Furthermore, we define an error metric as follows:

$$s_i = \dot{e}_i + K_{i2} e_i + K_{i1} \int_0^t e_i d\tau. \tag{56}$$

The time derivative description of the error metric is represented in the following formula:

$$\dot{s}_i = \ddot{e}_i + K_{i2} \dot{e}_i + K_{i1} e_i. \tag{57}$$

The solution to equation $\dot{s}_i = 0$, which is a homogeneous linear differential equation, describes the behavior of $e_i(t)$ which decays exponentially to zero [35]. Consequently, by maintaining this condition, asymptotically perfect tracking can be obtained.

The system with the controller uses the exact feedback linearization method and then applies $\boldsymbol{K}$, i.e., the feedback gain matrix represented in Equation (23), so that the following formula is obtained:

$$v_i = K_{i2} \dot{e}_i + K_{i1} e_i \tag{58}$$

will imply $\dot{s}_i = 0$.

The system with the controller uses the approximating feedback linearization method and then applies $\boldsymbol{L}$, i.e., the feedback gain matrix represented in Equation (50), so that the following formula is obtained:

$$T_1 = L_{11} e_1 + L_{12} \dot{\theta}_1 + L_{13} \theta_2 + L_{14} \dot{\theta}_2,$$
$$T_2 = L_{21} \theta_1 + L_{22} \dot{\theta}_1 + L_{23} e_2 + L_{24} \dot{\theta}_2, \tag{58}$$

will imply:

$$\dot{s}_i = \Delta_i. \tag{59}$$

Let us define a_{i1}^*, a_{i2}^*, and b_i^* such that:

$$\dot{s}_i = a_{i2}^* \dot{e}_i + a_{i1}^* e_i + b_i^* T_i, \tag{60}$$

where a_{i1}^*, a_{i2}^*, and b_i^* are unknown real positive numbers.

Assumption 1

The control gain, b_i^*, is the globally bounded strictly positive gain, which is the largest limit of the control gain, which varies from zero until it reaches an unknown value $\underline{b_i}$, such that $b_i^* \geq \underline{b_i} > 0$.

When a_{i1}^*, a_{i2}^*, and b_i^* are known exactly, to satisfy control purposes, the proposed control law is described using the following formula:

$$T_i = -\frac{1}{b_i^*}(a_{i2}^*\dot{e}_i + a_{i1}^*e_i + \alpha_i b_i^* s_i), \quad (61)$$

$$T_i = -\frac{1}{b_i^*}(a_{i2}^*\dot{e}_i + a_{i1}^*e_i + \alpha_i b_i^* s_i), \quad (62)$$

where α_i is a positive constant, which is a design parameter.

By substituting Equation (61) into Equation (60), we get the following equation:

$$\dot{s}_i = -\alpha_i b_i^* s_i. \quad (63)$$

The candidate for the designed Lyapunov function is formulated as follows:

$$V = \frac{1}{2}s_i^2, \quad (64)$$

then:

$$\dot{V} = s_i\dot{s}_i = -\alpha_i b_i^* s_i^2. \quad (65)$$

Utilizing the reality that $b_i^* \geq \underline{b_i} > 0$, we get:

$$\dot{V} \leq -\alpha_i \underline{b_i} s_i^2 \leq 0. \quad (66)$$

Thus, we can conclude that $s_i(t) \to 0$ as $t \to \infty$, and therefore $e_i(t) \to 0$ as $t \to \infty$ for $i = 1,\ 2$.

Equation (65) shows that if parameter α_i has a greater value, it will result in an increasingly negative value of $\dot{V}$. Therefore, the tracking error convergence rate can be adjusted by varying the value of α_i, which is a design parameter.

In this research, it is assumed that the values of parameters a_{i1}^*, a_{i2}^*, and b_i^* are unknown, so it is impossible to obtain the control law (61). By considering this fact, we design a control system using an adaptive control method so that the control objectives are met. The approximations of the parameters are described using the representations $\hat{a}_{i1}$, $\hat{a}_{i2}$, and $\hat{b}_i$, respectively.

The parameter errors are defined by the following formula:

$$\tilde{a}_{i1} = a_{i1}^* - \hat{a}_{i1}, \quad (67)$$

$$\tilde{a}_{i2} = a_{i2}^* - \hat{a}_{i2}, \quad (68)$$

$$\tilde{b}_i = b_i^* - \hat{b}_i. \quad (69)$$

Assume that the system represented in (60) can approximate the uncertainty as the following:

$$a_{i1} = a_{i1}^* + \varepsilon_{i1}, \quad (70)$$

$$a_{i2} = a_{i2}^* + \varepsilon_{i2}, \quad (71)$$

$$b_i = b_i^* + \varepsilon_{bi}, \quad (72)$$

where ε_{i1}, ε_{i2}, and ε_{bi} are approximation errors, while a_{i1}^*, a_{i2}^*, and b_i^* are the ideal parameters that cause the functions $|\varepsilon_{i1}|$, $|\varepsilon_{i2}|$, and $|\varepsilon_{bi}|$ to be minimal, respectively.

Assumption 2

The reconstruction errors of parameters ε_{i1}, ε_{i2}, and ε_{bi} are bounded, i.e., $|\varepsilon_{i1}| < \bar{\varepsilon}_{i1}$, $|\varepsilon_{i2}| < \bar{\varepsilon}_{i2}$, and $|\varepsilon_{bi}| < \bar{\varepsilon}_{bi}$, where the upper bounds of the parameters are unknown constants, i.e., $\bar{\varepsilon}_{i1}$, $\bar{\varepsilon}_{i2}$, and $\bar{\varepsilon}_{bi}$.

Assumption 3

The ideal parameters are bounded by known positive values, i.e., $|a_{i1}| < M_{i1}$, $|a_{i2}| < M_{i2}$, and $|b_i| < M_i$, where $|a_{i1}| < M_{i1}$, M_{i2}, and M_i are given constants.

Based on the control law represented in Equation (61) and coupled with the parameter estimation developed above, the adaptive control law is proposed with the following formula:

$$T_i = T_i^{nom} + T_i^r. \tag{73}$$

The control law represented in Equation (72) is a combination of the nominal control part, T_i^{nom}, which is an approximation of the control law represented in Equation (61) using the estimated nominal uncertainty of the system, and the robustifying control part, T_i^r, which is designed to eliminate the effect of perturbation.

The nominal input control part, T_i^{nom}, is described by the following formula:

$$T_i^{nom} = \frac{\hat{b}_i}{\varepsilon_i^0 + \hat{b}_i^2}\left(\hat{a}_{i1}e_i + \hat{a}_{i2}\dot{e}_i + \alpha_i\hat{b}_i s_i\right), \tag{74}$$

where ε_i^0 indicates a small positive constant.

Remark 1

The nominal control law in Equation (73), in order to be well defined when $\hat{b}_i$ goes to zero, it is necessary to replace the value of $\hat{b}_i^{-1}$ with $\hat{b}_i/\left(\varepsilon_i^0 + \hat{b}_i^2\right)$, in such a way that this formula can be considered as a Levenberg–Marquard regularized inverse [50] which was implemented in a scalar function.

The robustifying control part, adopted from Labiod and Boucherit [50], is described as follows:

$$T_i^r = \frac{\psi_i s_i}{|s_i| + \delta_i^2 exp(-\psi_i)}, \tag{75}$$

where:

$$\psi_i = \hat{\varepsilon}_i + \hat{\varepsilon}_{bi}\left|T_i^{nom} - \alpha_i s_i\right| + \hat{\varepsilon}_{ui}\left|T_i^0\right|, \tag{76}$$

$$T_i^0 = \frac{\varepsilon_i^0}{\varepsilon_i^0 + b_i^2}\left(\hat{a}_{i1}e_i + \hat{a}_{i2}\dot{e}_i + \alpha_i\hat{b}_i s_i\right), \tag{77}$$

and $\hat{\varepsilon}_{\mathrm{i}}$, $\hat{\varepsilon}_{b\mathrm{i}}$, and $\hat{\varepsilon}_{u\mathrm{i}}$ are approximations of the unknown variables $\varepsilon_{\mathrm{i}}^* = (\bar{\varepsilon}_{1\mathrm{i}} + \bar{\varepsilon}_{2\mathrm{i}})/\underline{b_i}$, $\varepsilon_{b\mathrm{i}}^* = \bar{\varepsilon}_{b\mathrm{i}}/\underline{b_i}$, and $\varepsilon_{u\mathrm{i}}^* = 1/\underline{b_i}$ respectively, and δ_{i} is a variable designed with the time-varying method.

The adaptation method for the controller parameters is designed with the following formula:

$$\dot{\hat{a}}_{i1} = -\eta_{i1}e_i s_i - \Phi_{i1}, \tag{78}$$

$$\dot{\hat{a}}_{i2} = -\eta_{i2}\dot{e}_i s_i - \Phi_{i2}, \tag{79}$$

$$\dot{\hat{b}}_i = -\eta_i s_i(T_i^{nom} - \alpha_i s_i) - \Phi_i, \tag{80}$$

$$\dot{\hat{\varepsilon}}_i = \eta_0|\sigma|, \tag{81}$$

$$\dot{\hat{\varepsilon}}_{bi} = \eta_0|\sigma|\left|T_i^{nom} - \alpha\sigma\right|, \tag{82}$$

$$\dot{\hat{\varepsilon}}_u = \eta_0|\sigma|\left|T_i^0\right|, \tag{83}$$

$$\dot{\delta} = -\eta_0\delta, \tag{84}$$

where $\eta_{\mathrm{i1}} > 0, \eta_{\mathrm{i2}} > 0, \eta_{\mathrm{i}} > 0, \eta_0 > 0, \delta(0) > 0, \Phi_{\mathrm{i1}}, \Phi_{\mathrm{i2}}$, and Φ_{i} is defined as follows:

$$\Phi_{i1} = \begin{cases} 0 & if\ |a_{i1}| < M_{i1}, \\ \eta_{i1}\rho_0\dfrac{|a_{i1}e_i s_i|}{a_{i1}} & otherwise, \end{cases} \tag{85}$$

$$\Phi_{i2} = \begin{cases} 0 & if\ |a_{i2}| < M_{i2}, \\ \eta_{i2}\rho_0\dfrac{|a_{i2}e_i s_i|}{a_{i2}} & otherwise, \end{cases} \tag{86}$$

$$\Phi_i = \begin{cases} 0 & if\ |b_i| < M_i, \\ \eta_i\rho_0\dfrac{|s_i(T_i^{nom} - \alpha_i s_i)|}{b_i} & otherwise, \end{cases} \tag{87}$$

where $\rho_0 \geq 1$.

Next, we will carry out the proof of the theorem discussed below.

Theorem 3

Examine the control law in Equation (72). If all assumptions in 1-3 can be fulfilled, the system uses the control law expressed in Equation (73), that is, the nominal controller, and then, combined with the adaptation law described by the formula in Equations (77)–(83), the result for the whole system will be able to guarantee the following properties:

1) It can be proven that the estimated values of all parameters are bounded and at any time the values fulfill $|a_{i1}| < M_{i1}$, $|a_{i2}| < M_{i2}$, and $|b_i| < M_i$.
2) All state variables and the manipulated variable will be bounded, i.e., $\theta,\ u \in L_\infty$.
3) Decreasing values for tracking errors and their derivatives will, at least, be asymptotically towards zero, i.e., $e_i(t) \to 0$ as $t \to \infty$ for $i = 1,\ 2$.

Proof

To validate that $|a_{i1}| < M_{i1}$, we will define a Lyapunov function as follows:

$$V_{i1} = \frac{1}{2} a_{i1}^2. \tag{88}$$

Then:

$$\dot{V}_{i1} = a_{i1} \dot{a}_{i1}. \tag{89}$$

Implementing the adaptation law in Equation (77) will change Equation (88) to be as follows:

$$\dot{V}_f = -\eta_{i1} a_{i1} e_i s_i - a_{i1} \Phi_{i1}. \tag{90}$$

For the case $|a_{i1}| > M_{i1}$ and using (84) one can obtain:

$$\dot{V}_{i1} = -\eta_{i1} a_{i1} e_i s_i - \eta_{i1} \rho_0 |a_{i1} e_i s_i|, \tag{91}$$

which can be simplified to:

$$\dot{V}_{i1} \le -\eta_{i1} (\rho_0 - 1) |a_{i1} e_i s_i|. \tag{92}$$

Because $\rho_0 \ge 1$ by definition, thus, $\dot{V}_f \le 0$, and one concludes that $|a_{i1}| < M_{i1}$, will always be fulfilled for all time if we select $\|a_{i1}(0)\| \le M_{i1}$. In the same way, one can prove that $|a_{i2}| < M_{i2}$ and $|b_i| < M_i$.

By utilizing the control law stated in (72), Equation (60) can be re-described as follows:

$$\dot{s}_i = a_{i2}^* \dot{e}_i + a_{i1}^* e_i + b_i^* T_i^{nom} + b_i^* T_i^r, \tag{93}$$

which will be described with the following representation:

$$\dot{s}_i = a_{i2}^* \dot{e}_i + a_{i1}^* e_i + (b_i^* - \hat{b}_i) T_i^{nom} - \hat{b}_i T_i^{nom} + b_i^* T_i^r. \tag{94}$$

By utilizing (73), we represent the following equation:

$$\dot{s}_i = (a_{i2}^* - \hat{a}_{i2}) \dot{e}_i + (a_{i1}^* - \hat{a}_{i1}) e_i + (b_i^* - \hat{b}_i) T_i^{nom} + b_i^* T_i^r - \alpha_i \hat{b}_i s_i. \tag{95}$$

Adding and subtracting $\alpha_i b_i^* s_i$ in (91), we can write:

$$\dot{s}_i = -\alpha_i b_i^* s_i + (a_{i2}^* - \hat{a}_{i2}) \dot{e}_i + (a_{i1}^* - \hat{a}_{i1}) e_i + (b_i^* - \hat{b}_i)(T_i^{nom} + \alpha_i s_i) + b_i^* T_i^r. \tag{96}$$

With (66)–(68), (95) becomes:

$$\dot{s}_i = -\alpha_i b_i^* s_i + \tilde{a}_{i2} \dot{e}_i + \tilde{a}_{i1} e_i + \tilde{b}_i (T_i^{nom} + \alpha_i s_i) + b_i^* T_i^r. \tag{97}$$

And then, to assure the remainder of Theorem 3, we develop the following candidate Lyapunov-like function:

$$V = \frac{1}{2} s_i^2 + \frac{1}{2\eta_{i1}} \tilde{a}_{i1}^2 + \frac{1}{2\eta_{i2}} \tilde{a}_{i2}^2 + \frac{1}{2\eta_i} \tilde{b}_i^2 + \frac{b_i}{2\eta_0} \tilde{\varepsilon}_i^2 + \frac{b_i}{2\eta_0} \tilde{\varepsilon}_{bi}^2 + \frac{b_i}{2\eta_0} \tilde{\varepsilon}_u^2 + \frac{b_i}{2\eta_0} \delta^2, \tag{98}$$

where $\tilde{\varepsilon}_i = \varepsilon_i^* - \hat{\varepsilon}_i$, $\tilde{\varepsilon}_{bi} = \varepsilon_{bi}^* - \hat{\varepsilon}_{bi}$, and $\tilde{\varepsilon}_u = \varepsilon_u^* - \hat{\varepsilon}_u$.

The time derivative of (97) is:

$$\dot{V} = s_i \dot{s}_i - \frac{1}{\eta_{i1}} \tilde{a}_{i1} \dot{\hat{a}}_{i1} - \frac{1}{\eta_{i2}} \tilde{a}_{i2} \dot{\hat{a}}_{i2} - \frac{1}{\eta_i} \tilde{b}_i \dot{\hat{b}}_i - \frac{b_i}{\eta_0} \tilde{\varepsilon}_i \dot{\hat{\varepsilon}}_i - \frac{b_i}{\eta_0} \tilde{\varepsilon}_{bi} \dot{\hat{\varepsilon}}_{bi} - \frac{b_i}{\eta_0} \tilde{\varepsilon}_u \dot{\hat{\varepsilon}}_u + \frac{b_i}{\eta_0} \delta \dot{\delta}. \tag{99}$$

With (96), (98) becomes:

$$\dot{V} = -\alpha_i b_i^* s_i^2 + \dot{V}_1 + \dot{V}_2, \tag{100}$$

where:

$$\dot{V}_1 = -\tilde{a}_{i1} e_i s_i - \tilde{a}_{i2} \dot{e}_i s_i - \tilde{b}_i s_i (T_i^{nom} - \alpha_i s_i) - \frac{1}{\eta_{i1}} \tilde{a}_{i1} \dot{\hat{a}}_{i1} - \frac{1}{\eta_{i2}} \tilde{a}_{i2} \dot{\hat{a}}_{i2} - \frac{1}{\eta_i} \tilde{b}_i \dot{\hat{b}}_i, \tag{101}$$

$$\dot{V}_2 = -\alpha_i b_i^* T_i^r + s_i T_i^0 - \alpha_i \varepsilon_{i1} - \alpha_i \varepsilon_{i2} - s_i \varepsilon_i (T_i^{nom} - \alpha_i s_i) - \frac{\underline{b_i}}{\eta_0} \tilde{\varepsilon}_i \dot{\hat{\varepsilon}}_i - \frac{\underline{b_i}}{\eta_0} \tilde{\varepsilon}_{bi} \dot{\hat{\varepsilon}}_{bi} - \frac{\underline{b_i}}{\eta_0} \tilde{\varepsilon}_u \dot{\hat{\varepsilon}}_u + \frac{\underline{b_i}}{\eta_0} \delta \dot{\delta}. \quad (102)$$

Using (77)–(79), (100) becomes:

$$\dot{V}_1 = \tilde{a}_{i1} \Phi_{i1} + \tilde{a}_{i2} \Phi_{i2} + \tilde{b}_i \Phi_i. \quad (103)$$

Let us now prove that $\tilde{a}_{i1} \Phi_{i1} \leq 0$. If $|\hat{a}_{i1}| \leq M_{i1}$, $\Phi_{i1} = 0$, the conclusion is trivial. For $|\hat{a}_{i1}| \geq M_{i1}$, since $|a_{i1}^*| \leq M_{i1}$, one has $2\tilde{a}_{i1} \hat{a}_{i1} = |a_{i1}^*|^2 - |\hat{a}_{i1}|^2 - |a_{i1}^* - \hat{a}_{i1}|^2 \leq 0$. Thus $\tilde{a}_{i1} \Phi_{i1} = \tilde{a}_{i1} \frac{|\hat{a}_{i1} e_i s_i|}{\hat{a}_{i1}} \leq 0$. In the same way, we can prove that $\tilde{a}_{i2} \Phi_{i2} \leq 0$ and $\tilde{b}_i \Phi_i \leq 0$. From the previous results, it can be concluded with the following formula:

$$\dot{V}_1 \leq 0. \quad (104)$$

The boundedness of Equation (101) can be represented as follows:

$$\dot{V}_2 \leq \underline{b_i} |s_i| \{ \varepsilon_u^* |u_0| + \varepsilon_i^* + \varepsilon_{bi}^* |T_i^{nom} - \alpha_i s_i| \} - s_i b_i^* T_i^r - \frac{\underline{b_i}}{\eta_0} \tilde{\varepsilon}_i \dot{\hat{\varepsilon}}_i - \frac{\underline{b_i}}{\eta_0} \tilde{\varepsilon}_{bi} \dot{\hat{\varepsilon}}_{bi} - \frac{\underline{b_i}}{\eta_0} \tilde{\varepsilon}_u \dot{\hat{\varepsilon}}_u + \frac{\underline{b_i}}{\eta_0} \delta \dot{\delta}. \quad (105)$$

From (75), (76), (80)–(83), (104) can be bounded as:

$$\dot{V}_2 \leq \underline{b_i} \delta^2 \psi \, exp(-\psi) + \frac{\underline{b_i}}{\eta_0} \delta \dot{\delta}. \quad (106)$$

From (83) and using the fact that $\psi \, exp(-\psi) \leq 1$, (105) can be reduced to:

$$\dot{V}_2 \leq 0. \quad (107)$$

From (103), (106), and Assumption 1, (99) becomes:

$$\dot{V} \leq -\alpha_i \underline{b_i} s_i^2. \quad (108)$$

Finally, $V \in L_\infty$, which shows the boundedness of the signals $s_i(t)$, $\tilde{a}_{i1}(t)$, $\tilde{a}_{i2}(t)$, $\tilde{b}_i(t)$, $\tilde{\varepsilon}_{i1}(t)$, $\tilde{\varepsilon}_{i2}(t)$, $\tilde{\varepsilon}_{bi}(t)$, $\tilde{\varepsilon}_u(t)$, and $\delta(t)$. The implication of this, in turn, causes the signals $\theta_i(t)$, $T_i(t)$, and $\dot{s}_i(t)$ to be bounded.

4. Simulation Result and Discussion

The parameters of the manipulator robot in the simulation process are nominally determined as follows: $m_1 = 4\ kg$, $m_2 = 2\ kg$, $l_1 = 1\ m$, $l_2 = 0.5\ m$, $g = 9.8\ N/kg$. In this paper, the robotic manipulator is desired to take the load from position one ($\theta_1 = 0.5$ rad and $\theta_2 = 1$ rad) to position two ($\theta_1 = 1$ rad and $\theta_2 = 2$ rad). In the first stage, the robotic manipulator shifts from the initial position to position 1 along a predetermined path for 2 seconds. It stays there for 1 s to take the load ($m_{load} = 1\ kg$) and starts to shift from position one to position two at $t = 3$ s. In the second stage, a perturbation ($t_1 = t_1 + 1000\ N$) is added to link 1 at $t = 3.8$ s and eliminated at $t = 4$ s. From the explanation above, in total there are three dynamic turnarounds in the whole process activated by enlarging the load, entering the perturbation, and returning to normal when the perturbation is eliminated.

The resulting simulations are depicted in Figures 2–6. As manifested in Figure 2 and Figure 3, the joint angles follow the prescribed path, and the developed controller forces the robotic manipulator to the prescribed position.

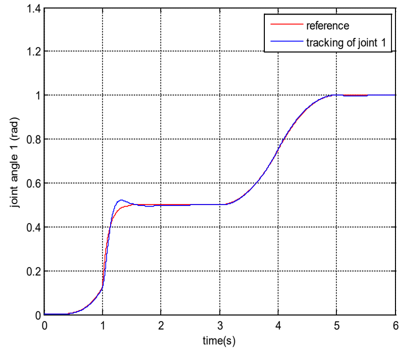

Figure 2. Tracking of joint 1 with the proposed controller.

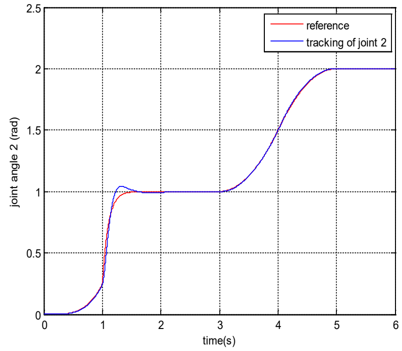

Figure 3. Tracking of joint 2 with the proposed controller.

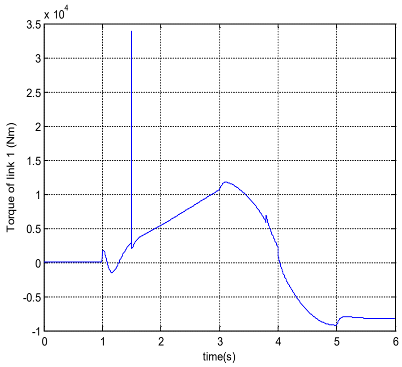

Figure 4. Control torque of joint 1 with the proposed controller.

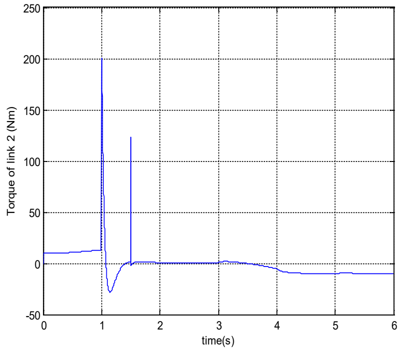

Figure 5. Control torque of joint 2 with the proposed controller

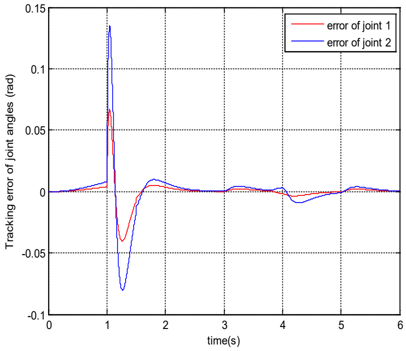

Figure 6. Tracking error of joint angles with the proposed controller

5. Conclusions

The developed controller technique is synthesized in five stages. In the first stage, the exact linearization using feedback is developed. In the second stage, the controller candidate designed by approximating the exact feedback controller is applied to the plant to replace the exact controller. In the third stage, the validation of the Lyapunov stability criteria for the candidate controller was carried out. In the fourth stage, the implementation of data-driven, robust adaptive control is realized. In the fifth stage, digital simulation is used to realize the candidate controller implementation.

The advantage of the designed controller is that it can apply well-established theory about robust adaptive control and the ease of application of an approximating state feedback controller. The developed adaptive control could push the robot manipulator to its prescribed path. The effectiveness of the developed adaptive control scheme is verified using digital simulations.

6. References

[1]. S. Yurkovich, *Flexibility Effects on Performance and Control, Robot Control*. New York: IEEE Press, 1992.

[2]. S. Anwari, "Implementation of Neurofuzzy Controller to Robot Manipulator," 2004.

[3]. D. Mahayana, "Synthesis of Approximating State Feedback for Robotic Manipulator," 2011.

[4]. D. Mahayana and S. Anwari, "Robust Adaptive Proportional Integral Sliding Mode Control Based on Synthesis of Approximating State Feedback for Robotic Manipulator," in *2018 IEEE 8th International Conference on System Engineering and Technology (ICSET)*, IEEE, Oct. 2018, pp. 195–200. doi: 10.1109/ICSEngT.2018.8606370.

[5]. D. Mahayana and S. Anwari, "Robust adaptive control for robotic manipulator based on chattering free variable structure system," in *2009 International Conference on Electrical Engineering and Informatics*, IEEE, Aug. 2009, pp. 247–252. doi: 10.1109/ICEEI.2009.5254779.
[6]. D. Mahayana, "Sliding mode control based on synthesis of approximating state feedback for robotic manipulator," *International Journal on Electrical Engineering and Informatics*, vol. 9, no. 3, pp. 504–520, Sep. 2017, doi: 10.15676/ijeei.2017.9.3.7.
[7]. N. Sadati and R. Ghadami, "Adaptive multi-model sliding mode control of robotic manipulators using soft computing," *Neurocomputing*, vol. 71, no. 13–15, pp. 2702–2710, Aug. 2008, doi: 10.1016/j.neucom.2007.06.019.
[8]. N. Sadati, R. Ghadami, and M. Bagherpour, "A Robust Adaptive Neural Network Controller Based on Variable Structure System," 2005.
[9]. R. Gholipour and M. M. Fateh, "Robust Control of Robotic Manipulators in the Task-Space Using an Adaptive Observer Based on Chebyshev Polynomials," *J Syst Sci Complex*, vol. 33, no. 5, pp. 1360–1382, Oct. 2020, doi: 10.1007/s11424-020-8186-0.
[10]. X. Ding, H. Wang, Y. Ren, Y. Zheng, C. Chen, and J. He, "Safety-Critical Optimal Control for Robotic Manipulators in A Cluttered Environment," Nov. 2022, [Online]. Available: http://arxiv.org/abs/2211.04944
[11]. R. Prakash, L. Behera, S. Mohan, and S. Jagannathan, "Dual-Loop Optimal Control of a Robot Manipulator and Its Application in Warehouse Automation," *IEEE Transactions on Automation Science and Engineering*, vol. 19, no. 1, pp. 262–279, Jan. 2022, doi: 10.1109/TASE.2020.3027394.
[12]. J. A. Rojas-Quintero, F. Dubois, and H. C. Ramírez-de-Ávila, "Riemannian Formulation of Pontryagin's Maximum Principle for the Optimal Control of Robotic Manipulators," *Mathematics*, vol. 10, no. 7, p. 1117, Mar. 2022, doi: 10.3390/math10071117.
[13]. S. Wang, K. Zhang, and G. Herrmann, "An Adaptive Controller for Robotic Manipulators with Unknown Kinematics and Dynamics," *IFAC-PapersOnLine*, vol. 53, no. 2, pp. 8796–8801, 2020, doi: 10.1016/j.ifacol.2020.12.1385.
[14]. A. Lotfazar, M. Eghtesad, and M. Mohseni, "Integrator backstepping control of a 5 DoF robot manipulator incorporating actuator dynamics," in *Proceedings of 2003 IEEE Conference on Control Applications, 2003. CCA 2003.*, IEEE, pp. 1007–1012. doi: 10.1109/CCA.2003.1223148.
[15]. B. Brahmi, M. Saad, C. El-Bayeh, M. H. Rahman, and A. Brahmi, "Novel adaptive backstepping control for uncertain manipulator robots using state and output feedback," *Robotica*, vol. 40, no. 5, pp. 1326–1344, May 2022, doi: 10.1017/S0263574721001132.
[16]. X. Cheng, Y. Zhang, H. Liu, D. Wollherr, and M. Buss, "Adaptive neural backstepping control for flexible-joint robot manipulator with bounded torque inputs," *Neurocomputing*, vol. 458, pp. 70–86, Oct. 2021, doi: 10.1016/j.neucom.2021.06.013.
[17]. C. Wang, "Adaptive RBF Neural Network Backstepping Control for Two-Link Robot Manipulators," *J Phys Conf Ser*, vol. 2283, no. 1, p. 012006, Jun. 2022, doi: 10.1088/1742-6596/2283/1/012006.
[18]. S. Yi, K. Watanabe, and I. Nagai, "Backstepping-based Super-Twisting Sliding Mode Control for a Quadrotor Manipulator with Tiltable Rotors," *Journal of Robotics and Control (JRC)*, vol. 3, no. 2, pp. 128–137, Feb. 2022, doi: 10.18196/jrc.v3i2.13368.
[19]. Z. Dachang, D. Baolin, Z. Puchen, and W. Wu, "Adaptive Backstepping Sliding Mode Control of Trajectory Tracking for Robotic Manipulators," *Complexity*, vol. 2020, pp. 1–11, Aug. 2020, doi: 10.1155/2020/3156787.
[20]. A. M. Abdul-Sadah, K. M. H. Raheem, and M. M. S. Altufaili, "A fuzzy logic controller for a three links robotic manipulator," 2022, p. 050026. doi: 10.1063/5.0066871.
[21]. L. Jin, S. Li, J. Yu, and J. He, "Robot manipulator control using neural networks: A survey," *Neurocomputing*, vol. 285, pp. 23–34, Apr. 2018, doi: 10.1016/j.neucom.2018.01.002.
[22]. D. Galvan-Perez, H. Yañez-Badillo, F. Beltran-Carbajal, I. Rivas-Cambero, A. Favela-Contreras, and R. Tapia-Olvera, "Neural Adaptive Robust Motion-Tracking Control for

Robotic Manipulator Systems," *Actuators*, vol. 11, no. 9, p. 255, Sep. 2022, doi: 10.3390/act11090255.
[23]. A. Carron, E. Arcari, M. Wermelinger, L. Hewing, M. Hutter, and M. N. Zeilinger, "Data-Driven Model Predictive Control for Trajectory Tracking With a Robotic Arm," *IEEE Robot Autom Lett*, vol. 4, no. 4, pp. 3758–3765, Oct. 2019, doi: 10.1109/LRA.2019.2929987.
[24]. X. Zhu, C. Ding, C. Ren, T. Zhang, L. Jia, and L. Wu, "Implementation of a robust data-driven control approach for an ommi-directional mobile manipulator based on koopman operator," *Measurement and Control*, vol. 55, no. 9–10, pp. 1143–1154, Nov. 2022, doi: 10.1177/00202940221094843.
[25]. Dimitri Mhayana, Sabat Anwari, and A. N. Putri, "Robust Chattering Free Data Driven Direct Adaptive Neuro Sliding Mode Control for Distillation Column," 2023.
[26]. Dimitri Mahayana and Sabat Anwari, "Data-Driven Proportional Integral Controller Based on Synthesis of Approximating State Feedback for Satellite Attitude Control," 2023.
[27]. R. Paolini and M. T. Mason, "Data-driven statistical modeling of a cube regrasp," in *2016 IEEE/RSJ International Conference on Intelligent Robots and Systems (IROS)*, IEEE, Oct. 2016, pp. 2554–2560. doi: 10.1109/IROS.2016.7759397.
[28]. D. Espinosa, S. Pacheco, J. C. Tejada, and T. Manrique, "Comparing Data-Driven motion tracking controllers for a Flexible-Joint Robotic Manipulator," in *2021 IEEE 5th Colombian Conference on Automatic Control (CCAC)*, IEEE, Oct. 2021, pp. 280–285. doi: 10.1109/CCAC51819.2021.9633281.
[29]. W. Sirichotiyakul, "Data-Driven Passivity-Based Control of Underactuated Robotic Systems," Boise State University, Boise, ID, 2022. doi: 10.18122/td.1997.boisestate.
[30]. M. G. Safonov, S. Holmes, and A. C. Doyle, "Data-Driven Robust Control Design: Unfalsified Control. "[Online]. Available: http://www.rto.nato.int/abstracts.asp.
[31]. H. A. A. Fattah, "Input-output linearization of induction motors with magnetic saturation," in *Proceedings of the 2000 American Control Conference. ACC (IEEE Cat. No.00CH36334)*, IEEE, 2000, pp. 600–604 vol.1. doi: 10.1109/ACC.2000.878970.
[32]. A. Mokhtari, A. Benallegue, and B. Daachi, "Robust feedback linearization and GH/sub /spl infin// controller for a quadrotor unmanned aerial vehicle," in *2005 IEEE/RSJ International Conference on Intelligent Robots and Systems*, IEEE, 2005, pp. 1198–1203. doi: 10.1109/IROS.2005.1545112.
[33]. M. W. Spong and T. GroeneveldCoordinated, "An Experimental Evaluation of Riemannian Curvature Based Feedback Linearization For A Direct Drive Manipulator," 2007.
[34]. A. Isidori, *Nonlinear Control Systems*. London: Springer London, 1995. doi: 10.1007/978-1-84628-615-5.
[35]. J.-J. E. (Jean-J. E.) Slotine and W. Li, *Applied nonlinear control*. Prentice Hall, 1991.
[36]. Dimitri Mahayana, *Sistem pengaturan dengan mikroprosesor.* PAU Mikroelektronika, 1991.
[37]. I. S. Nurbambang and Dimitri Mahayana, *Penguat Instrumentasi*. PAU Mikroelektronika., 1990.
[38]. C.S. Rangan, G.R. Sarma, and Mani, *Instrumentation Devices and Systems*. New Delhi: Tata McGraw Hill, 1992.
[39]. P. R. Gray and R. G. Meyer, *Analysis and Design of Analog Integrated Circuits*. New York: John Wiley and Sons, 1977.
[40]. Chang Cheh, Yan Wang, and Guangxiong Wang, "Nonlinear decoupling control and exact linearization of induction motor drive using microprocessor," in *Proceedings IECON '91: 1991 International Conference on Industrial Electronics, Control and Instrumentation*, IEEE, 1991, pp. 707–711. doi: 10.1109/IECON.1991.239201.
[41]. M. Ogawa, H. Yamamoto, and T. Itoh, "Tracking Controller Design for a Nonlinear CSTR Using Linearization," *Proc. IECON*, 1991.
[42]. Dimitri Mahayana, "Sintesa Sistem Kontrol Nonlinier," Bandung Institute of Technology, 1998.

[43]. W. Sun, Y. Wang, and X. Zhai, “Adaptive Control Based on Recurrent Fuzzy Wavelet Neural Network and Its Application on Robotic Tracking Control,” 2006, pp. 1166–1171. doi: 10.1007/11760023_171.
[44]. J.L. Goldberg, *Marix Theory with Applications*. Singapore: McGraw Hill, 1992.
[45]. P. Lancaster and M. Tismenetsky, *The Theory of Matrices*. London: Academic Press, 1985.
[46]. H.K. Khalil, *Nonlinear Systems*. New York: Macmillan Pulishing Company, 1992.
[47]. J. La Salle and S. Lefschetz, *Stability by Lyapunov Direct Method*. New York: Academic Press, 1961.
[48]. C.T. Chen, *Linear System Theory and Design*. New York: Holt-Saunders International Editions, 1970.
[49]. W. A. Boothby, a*n Introduction to Differentiable Manifolds and Riemanian Geometry*. New York: Academic Press, 1975.
[50]. S. Labiod and M. S. Boucherit, “Indirect Fuzzy Adaptive Control of a Class of SISO Nonlinear Systems,” *The Arabian Journal for Science and Engineering*, vol. 31, Mar. 2006.

Dimitri Mahayana graduated from Bandung Institute of Technology (ITB) in 1989 with a Bachelor’s degree in Electrical Engineering with cumlaude/ honor predicate. In 1994, he finished his Master of Engineering in Electrical Engineering as well in Waseda University (Tokyo, Japan), with straight-A mark. In 1998, he got his doctoral degree in ITB with cum-laude predicate. Some of his research interests are nonlinear dynamical system, time varying system, control theory and convergence between control engineering and data science. He is currently a lecturer in School of Electrical Engineering and Informatics, Bandung Institute of Technology (ITB).

Sabat Anwari graduated from National Institute of Technology (ITENAS) in 1996 with a Bachelor’s degree in Electrical Engineering. In 1999, he finished his Master’s degree in Electrical Engineering as well in Bandung Institute of Technology. His research interests are linear and nonlinear control system, instrumentation system, intelligent system. He is currently a lecturer in National Institute of Technology in Bandung (ITENAS).